

ENVIRONMENTALLY FRIENDLY ELECTROLYTE FOR HYDROGEN EMBRITTLEMENT TESTING OF STEELS

¹ Josef DULIŠKOVIČ, ¹ Hana JIRKOVÁ, ¹ Josef KASL

¹ Research and Testing Institute Plzen Ltd., Pilsen, Czech Republic, EU, <u>duliskovic@vzu.cz</u>, <u>jirkova@vzu.cz</u>, <u>kasl@vzu.cz</u>

https://doi.org/10.37904/metal.2025.5123

Abstract

The growing concern for environmental sustainability in industrial processes has led to the development of an environmentally friendly electrolyte for hydrogen embrittlement testing of steels. In this study, a new electrolyte composed of sodium dihydrogen phosphate (NaH2PO4), disodium hydrogen phosphate (Na2HPO4), L-cysteine (C3H7NO2S), and citric acid (C6H8O7) was tested as an alternative to the conventional 0.5 N sulfuric acid (H2SO4) electrolyte combined with thiourea (CH4N2S). Samples made from ČSN 13 030 steel were subjected to electrolytic hydrogen charging for different durations. Subsequently, Charpy impact tests and fractographic analyses were performed, and the hydrogen content in the samples was measured. The results showed that the new electrolyte provides hydrogen charging effectiveness comparable to that of the conventional sulfuric acid-based electrolyte. This indicates that the new formulation presents a more sustainable and environmentally friendly alternative for hydrogen embrittlement testing, without the environmental drawbacks associated with traditional electrolytes.

Keywords: Hydrogen embrittlement, sustainable testing methods, Charpy impact test

1. INTRODUCTION

The urgent need to reduce greenhouse gas emissions—driven by environmental impacts and international commitments, including those of the European Union—is accelerating the transition away from fossil fuels. One promising alternative is hydrogen; particularly green hydrogen produced via water electrolysis using renewable energy sources [1]. Hydrogen is a flexible and clean energy carrier with potential uses in industry, transportation, and energy infrastructure. One proposed application is the gradual blending of hydrogen into existing natural gas pipelines as a transitional step toward decarbonization. As hydrogen gains importance, ensuring the reliability and safety of components in contact with it—such as pipelines and pressure vessels becomes essential. A major concern is hydrogen embrittlement (HE), the degradation of mechanical properties due to atomic hydrogen absorption [2]. HE is considered one of the most serious threats to the structural integrity of steels, typically reducing ductility while yield and tensile strengths remain largely unaffected. This phenomenon is linked to interactions between hydrogen and microstructural defects, such as dislocations and inclusions, which can promote crack initiation and propagation. To assess material resistance to HE, electrolytic hydrogen charging followed by Charpy impact testing is commonly used. In this process, hydrogen enters the steel through electrochemical reactions in acidic or alkaline electrolytes. Sulfuric acid (H₂SO₄) with thiourea (CH₄N₂S) is often used for acidic environments, as thiourea inhibits hydrogen recombination and increases the amount of atomic hydrogen available for absorption [3-5]. Although effective, such electrolytes pose environmental and safety concerns. H₂SO₄ is highly corrosive, and thiourea is toxic and potentially carcinogenic. Therefore, there is increasing interest in safer and more sustainable alternatives—yet only a few studies, such as Motta et al. [3], have explored this area. This study addresses that gap by evaluating an environmentally friendly electrolyte for hydrogen embrittlement testing.



2. EXPERIMENT

For hydrogen charging, an environmentally friendly electrolyte was prepared using a mixture of biodegradable and non-toxic components. Initially, 6.8 g of sodium dihydrogen phosphate (NaH₂PO₄) and 8.7 g of disodium hydrogen phosphate (Na₂HPO₄) were dissolved in approximately 900 mL of distilled water to produce a phosphate buffer. The pH of the solution was adjusted to the target range of 7.0-7.4. This buffer provides a stable and controlled environment for electrochemical reactions without the risk of aggressive corrosion. Subsequently, 0.5 g of L-cysteine (C₃H₇NO₂S) of 98 % purity, a naturally occurring amino acid with reducing properties, was added. It acts as an oxidation inhibitor and modifies the steel surface, thereby promoting the formation of atomic hydrogen [6-8]. Then, 1.0 g of citric acid (C₆H₈O₇) was introduced. As a natural chelating agent, it helps stabilize the pH and maintains an active metal surface by dissolving potential oxide layers. The solution was then topped up with distilled water to a final volume of 1 litre, and the pH was rechecked. The composition of the electrolyte was confirmed by Fourier-transform infrared spectroscopy (FT-IR) using a NICOLET 380 spectrometer. The electrolyte operates through electrochemical mechanisms: H⁺ ions, originating from citric acid and the buffer, are reduced at the cathode, forming atomic hydrogen (H). This atomic hydrogen either recombines to molecular hydrogen (H2) or diffuses into the steel lattice. Test specimens were machined from ČSN 13 030 steel into standard Charpy V-notch geometry (2 mm) with dimensions of 10 mm × 5 mm × 55 mm. One group of samples was charged in the environmentally friendly electrolyte containing phosphate buffer, L-cysteine, and citric acid (denoted as FP+LC+KC), while the second group was charged in a conventional electrolyte consisting of 0.1 N sulfuric acid (H₂SO₄) with thiourea (CH₄N₂S). Charging was performed at room temperature. No voltage drop was observed during charging, indicating the good stability of stainless-steel electrodes. After charging, the specimens were fractured using an instrumented Charpy impact test. The hydrogen content was determined using an ONH analyser (LECO 836), and the fracture surfaces were examined by scanning electron microscopy (SEM) using a JEOL IT710HR instrument to evaluate microstructural features related to hydrogen embrittlement.

3. RESULTS AND DISCUSSION

3.1 Base Material Characterization

ČSN 13 030 is a low-carbon, Mn-alloyed structural steel used in welded pressure components such as boilers and piping. It provides a minimum tensile strength of 460 MPa and yield strength of 265 MPa, making it suitable for elevated temperature applications [9]. The as-received microstructure consists of a ferrite—pearlite mixture, with ferrite occupying 54.4 % and pearlite 45.6 % by volume (**Figure 1**). Grain sizes correspond to grades G = 6.5 (ferrite) and G = 5.5 (pearlite), according to ČSN EN ISO 643. Sulphide inclusions, mainly MnS, were observed. These serve as hydrogen traps—interfaces that can localize hydrogen, impeding its diffusion but increasing crack initiation risk under stress [10]. The hydrogen content in the uncharged material was measured at 1.78 ± 0.23 ppm using ONH analysis, consistent with expected values for this steel under normal storage conditions.

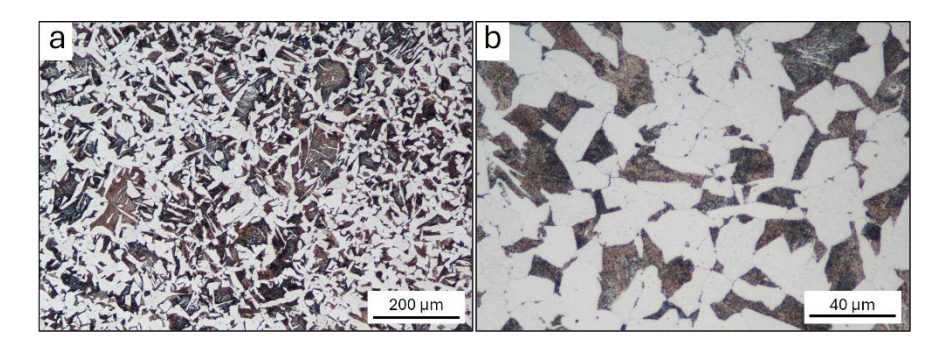


Figure 1 Microstructure of the base material, etched with 2 % Nital, showing a ferrite-pearlite structure.



3.2 FT-IR Spectroscopy

The FT-IR spectrum of the new electrolyte reveals several characteristic absorption bands corresponding to specific functional groups (Figure 2). A broad and intense band centred at 3280.8 cm⁻¹ is attributed to O-H stretching vibrations, primarily originating from water and hydroxyl groups of citric acid. The broadening of this band is due to extensive hydrogen bonding among water molecules and polar functional groups. Minor contributions from N-H stretching vibrations of the primary amine group in L-cysteine may also be present in this region. The band at 1633.8 cm⁻¹ is mainly associated with H–O–H bending vibrations of water molecules. This peak may partially overlap with C=O stretching modes of carboxylic groups present in both L-cysteine and citric acid. The absorption band at 1364.3 cm⁻¹ corresponds to CH₂ bending vibrations, likely arising from the methylene groups in L-cysteine and citric acid structures. A sharp band observed at 1086.8 cm⁻¹ is attributed to the asymmetric and symmetric stretching vibrations of phosphate groups (PO₄³⁻) from the phosphate buffer. The band at 989.5 cm⁻¹ is assigned to P-O bending modes, which further confirm the presence of phosphate species in the solution. In this region, minor overlapping contributions from C-O or S- containing groups (e.g., thiols) cannot be ruled out. Although S-H stretching vibrations of L-cysteine (typically expected around 2550 – 2600 cm⁻¹) are not clearly visible, they may be obscured by the dominant O-H band in the same region. In summary, the FT-IR spectrum reflects the expected chemical composition of the electrolyte, confirming the presence of water, phosphate ions, carboxylic acids, and amino acid-derived groups, all of which play key roles in the electrolyte's function and stability.

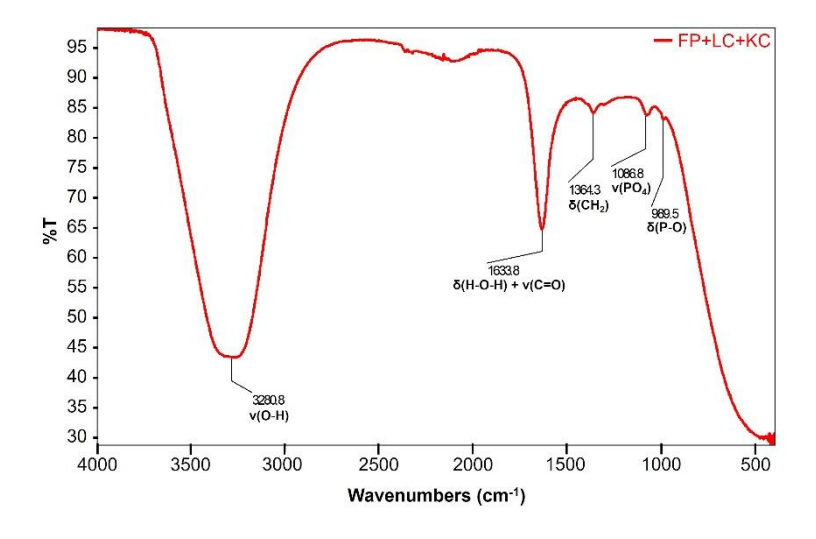


Figure 2 FT-IR Spectrum of the proposed electrolyte FP+LC+KC

3.3 Hydrogen Saturation

Figure 3 shows the increase in hydrogen content in ČSN 13 030 steel as a function of electrochemical charging time for two different electrolytes: the conventional $0.1N\ H_2SO_4$ solution and the newly developed environmentally friendly electrolyte (FP+LC+KC). Each data point represents the mean value from three independent measurements, with error bars indicating standard deviation. The initial hydrogen concentration prior to charging was measured at 1.78 ± 0.23 ppm, and this baseline is highlighted in the graph as a grey band. For the sulfuric acid electrolyte, the measured hydrogen content follows a characteristic saturation curve. The data were fitted using an exponential model of the form:

$$C(t) = C_{max}(1 - e^{-kt}) \tag{1}$$

where C(t) is the hydrogen content at time t (in ppm), C_{max} is the maximum equilibrium concentration (ppm), k is the rate constant (h⁻¹), and t is the charging time (in hours). This model is consistent with the expected behaviour of hydrogen absorption, where the uptake rate slows over time due to diffusion limitations and trap



saturation. The fit yielded $C_{max} = 9.71 \pm 7.24$ and $k = 0.068 \pm 0.064$ h⁻¹. Despite the good qualitative fit, the high uncertainty in C_{max} suggests significant variability, likely due to a limited number of sampling points and the steep gradient in early-stage absorption. In contrast, the FP+LC+KC electrolyte showed a linear increase in hydrogen content over the measured time interval (2, 5, and 15 hours). The data were fitted using a linear function:

$$C(t) = 0.288t + 0.55 \text{ with } R^2 = 0.998$$
 (2)

Where R^2 is coefficient of determination. This nearly perfect correlation suggests that saturation had not yet occurred during the experiment and that the hydrogen uptake rate remained constant. The lack of saturation may be attributed to slower hydrogen kinetics, either due to lower surface activity or a higher activation energy for diffusion into the steel. According to established hydrogen absorption models, it is expected that at longer charging times, the curve will begin to deviate from linearity and transition toward saturation. In summary, while the conventional H_2SO_4 -based electrolyte reaches saturation more quickly, the environmentally friendly FP+LC+KC system demonstrates a steady and effective hydrogen charging behaviour. Further long-term experiments will be necessary to determine the maximum hydrogen capacity and full saturation kinetics of the new electrolyte system.

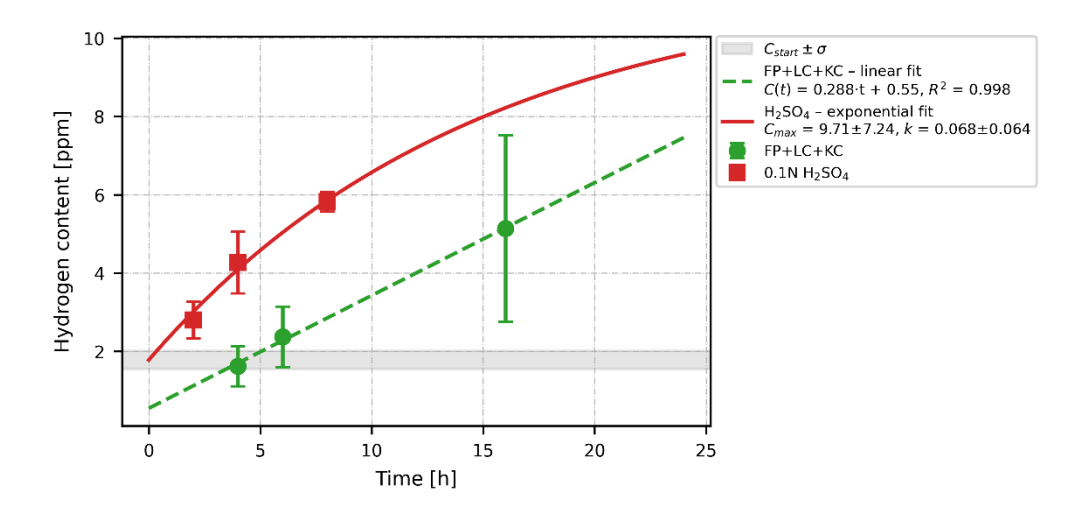


Figure 3 Dependence of hydrogen content on saturation time

3.4 Fractographic Analysis

From a macroscopic perspective, the fracture surface exhibits a mixed-mode character. It includes a ductile initiation zone below the notch, lateral shear lips, and a final fracture region also showing ductile morphology. These ductile zones border a central region of visually brittle, crystalline fracture morphology, which accounts for approximately 39 % of the total fracture surface area. The stable crack growth zone below the notch was primarily formed by trans granular ductile failure via a void coalescence mechanism. The fracture surface reveals dimples of three size categories: isolated large dimples (~ 20 µm), fine micro-meter scale dimples, and submicron-scale dimples located in tearing ligament regions (**Figure 4a**). Sporadically, small facets of trans granular cleavage and larger, curved facets typical of quasi-cleavage are observed. The central region associated with unstable crack propagation consists of alternating areas of predominantly trans granular cleavage and trans granular ductile tearing (**Figure 4b**). Tearing ligaments and curved quasi-cleavage facets are present throughout. **Figure 4c** shows a tearing ligament in detail, along with a large TTP-type dimple containing a brittle-fractured manganese sulphide (MnS) inclusion, which indicates hydrogen-assisted fracture initiation at inclusion sites. Cleavage areas are composed of flat facets ranging from 10 to 50 µm in size (**Figure 4d**). These are sometimes intersected by other facets propagating through pearlitic nodules, as captured in **Figure 4e**. In this figure, the crack crosses multiple nodules, and a transition from fan-like cleavage markings



to river patterns is evident. The final fracture region was produced primarily by trans granular shear tearing (**Figure 4f**), characterized by large dimples with a rough, rugged morphology. Fractographic observations also revealed a relatively high frequency of elongated sulphide inclusions, which tended to fracture in a brittle manner. In addition, distinct impressions of the underlying pearlitic microstructure were commonly visible on the fracture surface, indicating strong microstructural influence on crack propagation paths. The effect of hydrogen embrittlement was evident in the expansion of the brittle crystalline fracture zone, corresponding to a reduction in absorbed impact energy. This suggests that hydrogen contributed to matrix weakening and crack initiation, particularly at inclusion interfaces and regions of local stress concentration.

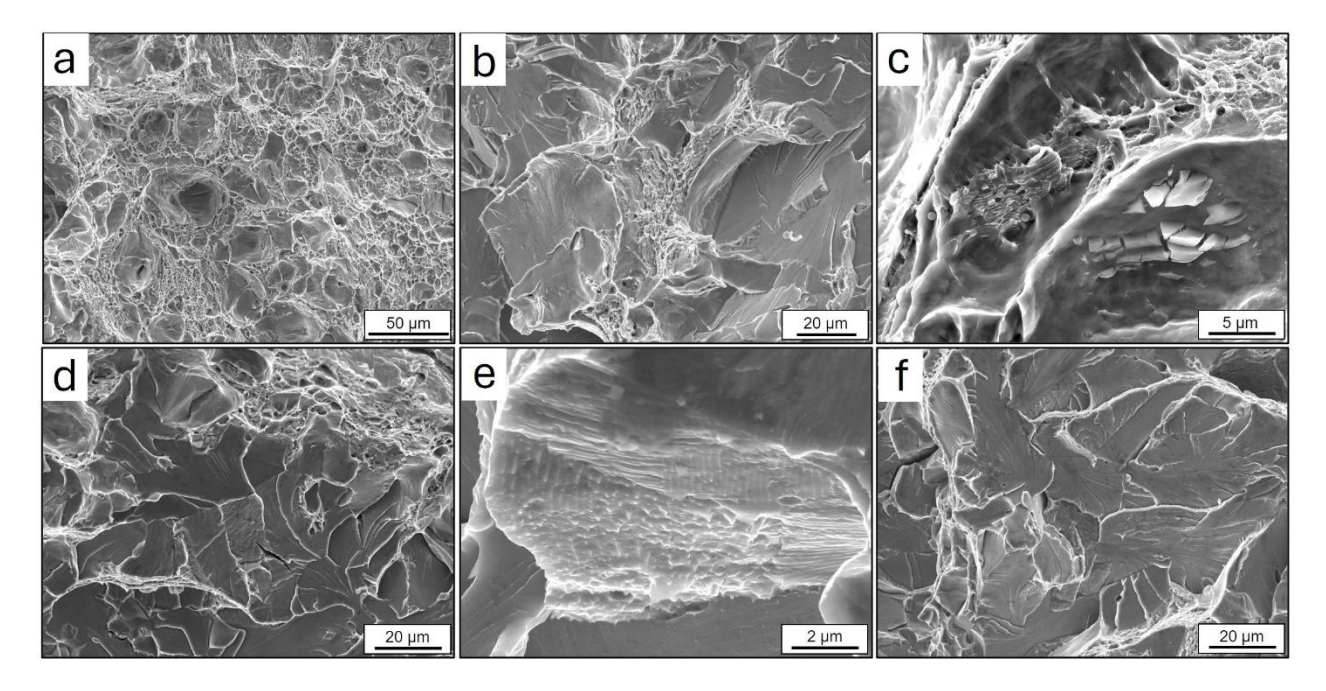


Figure 4 Fractographic analysis of a sample after 16 h hydrogen charging in the FP+LC+KC electrolyte.

4. CONCLUSION

This study presented the development and experimental validation of a new environmentally friendly electrolyte designed for hydrogen embrittlement testing of steels. The electrolyte, composed of phosphate buffer, L-cysteine, and citric acid, was developed as a sustainable alternative to the conventional electrolytes. The experiments confirmed that, despite its neutral pH and milder chemical composition, the FP+LC+KC electrolyte enabled effective hydrogen charging of ČSN 13 030 steel. Although full saturation was not achieved during the observed time frame and the hydrogen uptake exhibited a nearly linear trend, the results indicate stable and controlled kinetics, making the system well-suited for long-term charging experiments. In its current composition, the ecological electrolyte does not yet match the efficiency of the conventional H₂SO₄ based electrolyte, which reached saturation more rapidly. However, the FP+LC+KC formulation demonstrated consistent and reproducible hydrogen absorption and shows promise for achieving comparable hydrogen concentrations over extended charging durations. A major advantage of the new electrolyte lies in its minimal environmental and health impact. It contains no highly corrosive or toxic components, and all ingredients are biodegradable and safe for handling and disposal. Moreover, fractographic analysis confirmed that the electrolyte effectively induces features consistent with hydrogen embrittlement, including expanded brittle fracture zones and cleavage facets, thereby validating its functionality for embrittlement testing. The results suggest that the FP+LC+KC system represents a promising and safer alternative for hydrogen embrittlement testing, with potential applications in broader hydrogen-related technologies. Future research will focus on extending charging durations to evaluate saturation behaviour, exploring the applicability of the electrolyte to



other steel grades, and optimizing the formulation by investigating the effects of individual component concentrations to enhance hydrogen uptake performance and bring it closer to that of conventional systems.

ACKNOWLEDGEMENTS

The results were obtained within the HYGAS project No. SS06020165 co-funded with state support from the Environment for Life programme of the Technology Agency of the Czech Republic (TAČR) and the European Union NextGenerationEU within the National Recovery Plan.

REFERENCES

- [1] NOUSSAN, M., RAIMONDI, P.P., SCITA, R., HAFNER, M. The role of green and blue hydrogen in the energy transition—A technological and geopolitical perspective. Sustainability. 2021.
- [2] SINA, R., KIM, V., TOM, D., EDOARDO, P. Hydrogen embrittlement of pipeline steels under gaseous and electrochemical charging: A comparative review on tensile properties. *Engineering Failure Analysis*. 2025, vol. 167, ISSN 1350-6307.
- [3] MOTTA, D., DAMIN, A., DARJAZI, H., NEJROTTI, S., PICCIRILLI, F., BIRARDA, G., BAROLO, C., GERBALDI, C., ELIA, G.A., BONOMO, M. Eco-friendly NaCl glycerol-based deep eutectic electrolyte for high-voltage electrochemical double layer capacitor. *Green Chemistry*. 2025, ISSN 1463-9262.
- [4] MARGO, C., ROBIN D., WIM, D.W., STIJN, H., KIM, V., TOM, D. Effect of hydrogen charging on Charpy impact toughness of an X70 pipeline steel. *Procedia Structural Integrity*. 2022, Vol. 42, pp. 977-984, ISSN 2452-3216.
- [5] MARGO C., ROBIN D., WIM D.W., STIJN, H., TOM, D., KIM, V. Influence of electrochemical hydrogenation parameters on microstructures prone to hydrogen-induced cracking. *Journal of Natural Gas Science and Engineering*. 2022, Vol. 101, pp.104-533.
- [6] ALLESANDRO, C., FEDERICO U., ANTONIO, A., NICOLA, P. A review on hydrogen embrittlement and risk-based inspection of hydrogen technologies. *International Journal of Hydrogen Energy.* 2023, vol. 48, pp. 35316-35346, ISSN 0360-3199.
- [7] LI, Y., ZHANG, Z., LEE, D.J., QUANGUO, Z., YANYAN J., TIAN, Y., ZEXIAN, L. Role of L-cysteine and iron oxide nanoparticle in affecting hydrogen yield potential and electronic distribution in biohydrogen production from dark fermentation effluents by photo-fermentation. *Journal of Cleaner Production*. 2020, Vol. 276, pp. 123-193.
- [8] BILQEES, S., FAZLULLAH, K., KAMAL, N. Nonvitamin and Nonmineral Nutritional Supplements. *Academic Press*. 2019, pp. 53-58, ISBN 9780128124918.
- [9] ČSN 41 3030. Ocel 13 030 manganová. Praha: Český normalizační institut, 1986.
- [10] LUU, W.C., WU, J.K. Effects of sulfide inclusion on hydrogen transport in steels. *Materials Letters*. 1995, Vol. 24, No. 1–3, pp. 175-179.